A 1.7×4.1×2 mm³ Fully Integrated pH Sensor for Implantable Applications using Differential Sensing and Drift-Compensation

Taewook Kang[1], Inhee Lee[1], Sechang Oh[1], Taekwang Jang[2], Yejoong Kim[1], Hyochan Ahn[1], Gyouho Kim[1], Se-Un Shin[1], Seokhyeon Jeong[1], Dennis Sylvester[1], David Blaauw[1]

[1]University of Michigan, Ann Arbor, MI, USA; [2]ETH Zurich, Zurich, Switzerland

Abstract

This paper presents a 1.7×4.1×2 mm³ pH sensor that is a fully integrated, stand-alone and implantable system. Instead of a bulky cm size Ag/AgCl electrode, we use a mm-size integrated platinum electrode, and differential sensing using ISFET and REFET pair to compensate for unstable fluid potential. We also propose a drift compensation technique in which the leakage from the source and drain through the gate oxide is canceled, reducing drift >100×.

Introduction

Acidity of a fluid, expressed by its pH, plays a critical role in biochemical reactions and is a key sensing modality for biomedical applications, such as DNA sequencing and tumor health monitoring. pH sensing was revolutionized by the invention of the ion-sensitive field effect transistor (ISFET) [1], which enabled compact measurement of ion concentration and has become ubiquitous in pH sensing. However, to date, pH sensors have remained restricted to large benchtop equipment for laboratory use. While the ISFET itself is small, the fluid in which it is immersed must be at a known, well-controlled potential (V_{AQ}). The ISFET ion sensitivity then measures the potential relative to that of the fluid, providing the hydrogen ion concentration (Fig 1, top left). The industry standard method for controlling the fluid potential uses an Ag/AgCl reference electrode, which is cm-scale as it contains a liquid inside a thin glass vial. This raises the need for a mm-scale complete pH sensor to enable in-situ tissue monitoring and provide new insights into biochemical processes and enhance disease diagnosis.

Proposed System

This paper presents a 1.7×4.1×2 mm³ pH sensor that is fully integrated, including wireless communication, processor, battery, and energy management. Instead of a bulky Ag/AgCl electrode, we deposited a platinum electrode that measures only 50×60 μm². However, a metal electrode is known to produce an unstable fluid potential [1]. To address this, we augment the ISFET with a so-called reference FET (REFET), which is an ISFET with reduced sensitivity to pH. The REFET consists of an ISFET that is coated with 100 nm thickness parylene [2] (Fig. 1, right, bot). Since the ISFET and REFET exhibit the same sensitivity to fluid potential, the impact of its fluctuation on the ISFET can be subtracted using differential measurement (Fig. 1, top right). The proposed sensor integrates the platinum electrode, ISFET, and REFET into an area of only 1050×1380 μm² to create a mm-scale complete sensing system.

A second challenge in pH sensing is long-term drift of the ISFET floating-gate potential due to a gate leakage, which typically limits the lifespan of pH measurements to just minutes [3] (Fig. 2). This can be addressed by increasing the ISFET gate oxide thickness to > 10nm, but this restricts the readout circuits to relatively old technologies (0.350 μm and older) with poor transistor density. To enable pH sensing in a denser technology, we propose a dynamic drift compensation technique in which the leakage from the source and drain through the gate oxide is canceled, reducing drift from > 300mV/hour to 0.53mV/hour (differential output).

The proposed system consists of two identical sensing circuits, one for ISFET and one for REFET (Fig. 5). The floating gate of the ISFET is linearly dependent on pH (V_{GATE}=a-b(T)*pH) but cannot be directly observed. Hence, throughout its sensing operation, the sensing circuit places the ISFET in a constant-voltage-constant-current (CVCC) condition where I_D and V_{DS} are held constant (Fig. 3). In this condition, V_S tracks the floating gate V_G, and the circuit reads out the pH by sampling V_S through buffer A_2 using the 10-bit SAR ADC.

The cap-DAC in the SAR ADC is also used to maintain a constant V_{DS} across the ISFET, which together with the current source places it in the CVCC condition. This cap-DAC replaces the traditional resistor/current source in a conventional circuit [3] and reduces current consumption from μA to a few nA (Fig. 4). In addition, the cap-DAC allows the V_{DS} to be tuned, which enables compensation of the drift of the floating gate V_G, as explained below.

The floating gate experiences voltage drift due to the gate oxide leakage currents $I_{LK,SG}$ and $I_{LK,GD}$ (Fig. 6), which vary from device to device. Hence, the sensor first enters a calibration phase to cancel out this drift before sensing pH. $I_{LK,SG}$ and $I_{LK,GD}$ are strongly voltage dependent. Since the current is fixed in CVCC operation, V_{DS} can be tuned such that V_{GD} results in a balanced leakage, $I_{LK,SG}$=$I_{LK,GD}$, canceling the drift of V_G. During the calibration phase, the sensor is placed in a constant pH solution. The current source maintains $I_{D,const}$, while amplifier A_1 sets V_S as $V_{S,CAL}$ (=1.2V) by modulating V_D of the ISFET (Fig. 6, left configuration). If we assume V_G is initially zero, meaning the ISFET is in strong-inversion, the loop brings V_D close to $V_{S,CAL}$ to make V_{DS} small, which maintains $I_{D,const}$ with a large V_{GS}. Since V_S and V_D are higher than V_G, both leakage currents charge up the gate ($I_{LK,GD}$ is negative), and V_G will rise. As V_G increases and the ISFET enters weak-inversion, the loop will decrease V_D, which increases $I_{LK,GD}$. When $I_{LK,SG}$=$I_{LK,GD}$, V_S, V_G, and V_D settle and remain constant (t_1, Fig. 6). Hence, the proposed circuit automatically determines the drift-canceling condition by simply allowing the circuit to settle, which avoids complex search techniques. After it settles, the 10-bit SAR-ADC records V_{DS} at t_2 (=V_{DS}^*) (Fig. 6).

Following calibration, the circuit switches the configuration to pH sensing (Fig. 6, right). It now maintains V_{DS} using the same cap-DAC value that recorded V_{DS}^* during calibration. For example, when pH decreases (t_3), V_G increases, which in turn increases V_S. Amplifier A_2 drives voltage V_S on the cap-DAC, after which S_1 opens, S_2 closes, and the cap-DAC switches, shifting V_{DAC} by the previously recorder V_{DS}^* amount. Amplifier A_1 then sets V_D=V_{DAC}. Since pH change is much slower than the V_D refresh rate (156Hz), V_{DS} will remain essentially constant. The offset of A_1 cancels out since it impacts calibration and sensing equally. The offset of A_2 is pre-calibrated and subtracted from the cap-DAC code obtained during the calibration phase.

To readout pH, the ADC digitizes V_{DAC}=V_S (t_4, Fig. 6). The bottom plates of the cap-DAC are set to V_{DD} when sampling V_S to match their setting when maintaining V_{DS} (t_2). Since the V_{GS} of the ISFET in CVCC mode has temperature dependence, the bias-current $I_{D,const}$ is generated with constant V_{GS} voltage, creating intentional temperature modulation of $I_{D,const}$, which cancels variation of V_{GS} in the ISFET.

Measurement Results

The proposed pH sensor design was fabricated in 180-nm CMOS and integrated in a mm³-scale sensor node, including battery, power management, processor, radio, harvester, and solar cell and was fully functional (Fig. 7). The time-based measurement shows differential ADC code ($V_{S,ISFET}$–$V_{S,REFET}$) responding to pH change (Fig. 8). The ADC code plotted against a range of pH values shows a linear relationship (Fig. 10 top left), with a differential sensitivity of 7.86 LSB (9.7 mV)/pH. Fig. 10, top right, shows calibration mode operation, where the drain voltages of ISFET and REFET settle after 5 minutes. Using this recorded V_{DS} in CVCC operation, the drift rate of the source voltage decreased from 380 mV/hour without calibration to 3.4mV/hour in single ended mode and 0.53mV/hour in differential mode (Fig. 10 bot, left). Fig. 10 (bot, right) shows how the differential sensing effectively cancels out the noise of the liquid potential (V_{AQ}). The measured power is 176nW, and its distribution is shown in Fig. 11. The table 1 shows the comparison table. The proposed device marks the first fully integrated mm-scale pH-sensing device.

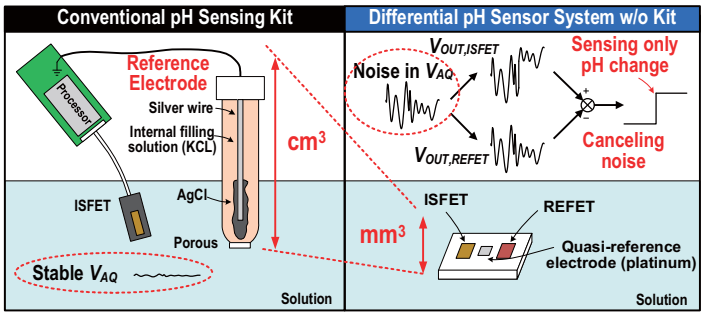

Fig. 2. Gate drift issue due to the unbalanced I_{LK}.

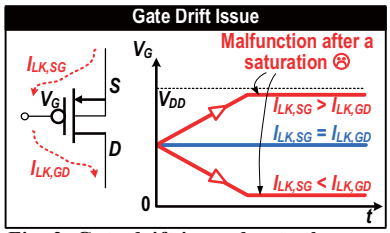

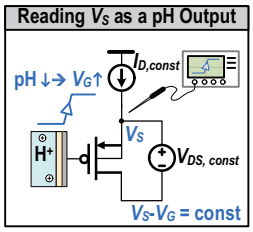

Fig. 3. CVCC description.

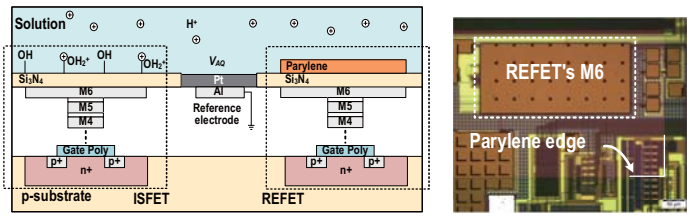

Fig.1. Motivation of removing the conventional reference electrode (top) and the structure of ISFET (bottom).

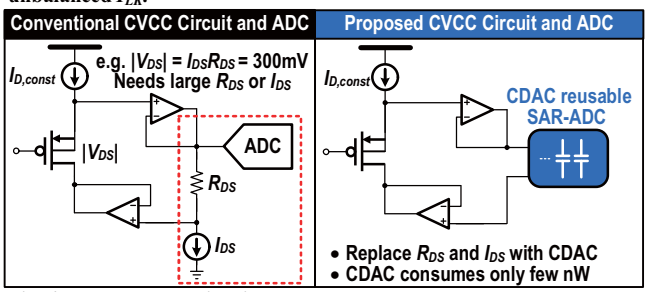

Fig. 4. The proposed circuit topology.

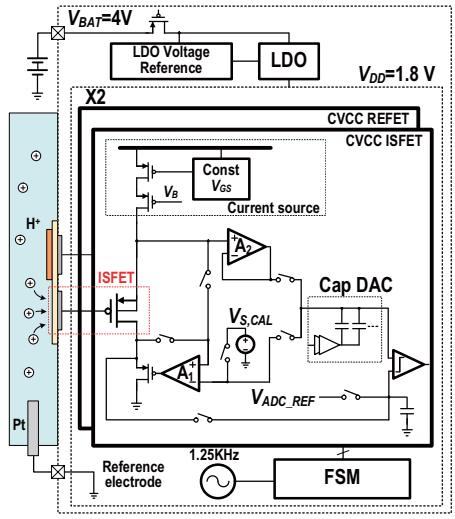

Fig. 5. Top circuit diagram.

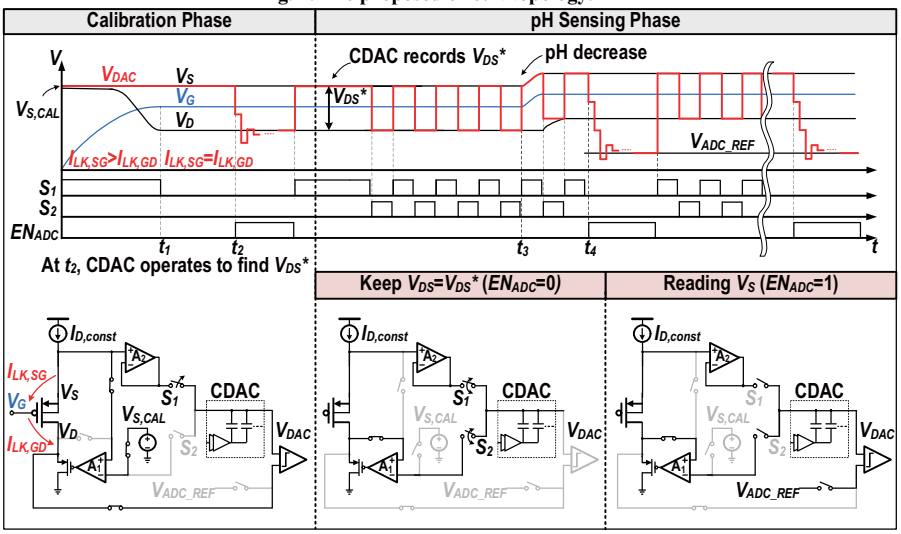

Fig. 6. Detailed explanation of the calibration and sensing phase.

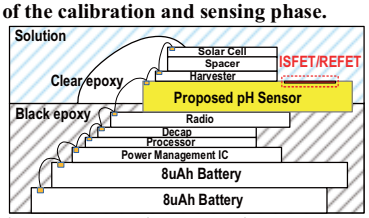

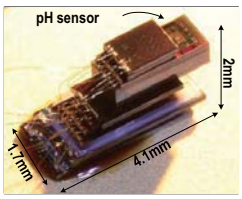

Fig 7. pH sensor integrated in a complete sensor system.

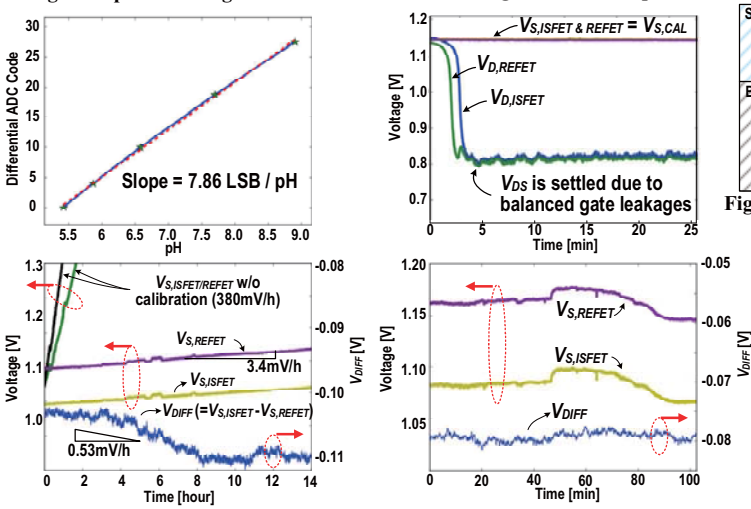

Fig. 10. Measurement results of pH sensitivity (top left), calibration phase (top right), and its result (bottom left), and common mode rejection in differential sensing (bottom right).

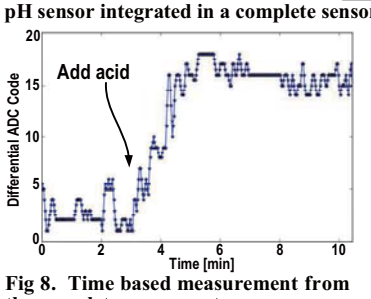

Fig 8. Time based measurement from the complete sensor system.

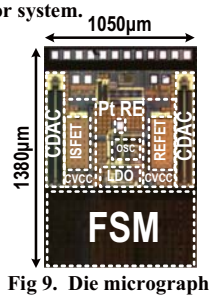

Fig 9. Die micrograph

References

[1] P. Bergveld, Sens. Act. B: Chem., 2003.
[2] T. Matsuo, et al., Sens. Act., 1984.
[3] P. A. Hammond, et al., IEEE TBME., 2005.
[4] M. Kalofonou, et al., IEEE TBioCAS., 2014.
[5] Y. Hu, et al., IEEE TBioCAS., 2014.
[6] W. P. Chan, et al., JSSC, Sep. 2010.

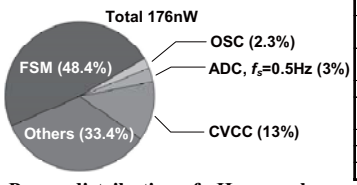

Fig. 11. Power distribution of pH sensor layer

Table1. Comparison table

	This Work	[4]	[5]	[6]
Technology	180nm	350nm	350nm	180nm
Reference Electrode	Platinum	Ag/AgCl	Ag/AgCl	Ag/AgCl
Topology	Differential CVCC with CDAC	Chemical Gilbert Cell	CVCC with reset	Current feedback with averaging
Sensitivity	7.86 LSB/pH	5.5nA/pH[c]	42.1mV/pH[d]	3KHz/pH[e]
Gate Drift Compensation	Yes	No need (large technology)	No need	No
Complete System	Yes	No	No	No
System Size[a]	1.7x4.1x2 mm³	N/A	N/A	N/A
Power	176nW[b]	165nW	848nW	76uW[f]

a. With sensing kit including RE
b. pH sensor layer described in Fig. 5
c, d. No following ADC
e. calculated from Fig. 15 and 18.
f. Excluding digital core